

## Periodical Morphodynamic Changes of Sand Movements at El Jadida Beach

Amine Bourhili<sup>1\*</sup>, Khalid El Khalidi<sup>1</sup>, Abdenaim Minoubi<sup>1</sup>, Mehdi Maanan<sup>2</sup>, Bendahhou Zourarah<sup>1</sup>

<sup>1</sup> Laboratory of Marine Geosciences and Soil Sciences, CNRST Associated Unit (URAC 45), Earth Sciences Department, Chouaib Doukkali University, El Jadida, Morocco

<sup>2</sup> Earth Sciences Department, Faculty of Sciences Ain Chock, Hassan II University of Casablanca, Casablanca, Morocco

\* Corresponding author's e-mail: aminebourhili@gmail.com

### ABSTRACT

El Jadida Beach (X: -8.5007116; Y: 33.2316326) is a sandy beach of low altitude that constitutes a kind of enclave located between the port of El Jadida and rocky outcrops. It is influenced by natural and anthropic factors, as well as the impact of tourism, particularly during the summer, when sand is used for amusement activities (Beach Ball competition). In order to follow the morphodynamic changes of this beach, we carried out a study on two different time scales: a fifty-five years (1963 – 2018) shoreline evolution study using aerial photos and satellite images based on GIS tools using the Digital Shoreline Analysis System (DSAS) and a two-years (2017–2019) morphological beach study using a Differential Global Positioning System (DGPS). According to the results obtained by the diachronic study, the beach studied showed erosion in its middle and an accumulation at these bulges. This result is due to the presence of the harbor breakwater to the NW and the rocky outcrops to the SE; acting as a barrier preventing the movement of sediments and the erosion in the middle can be explained by the reduction of the sediment supply from the Oued Oum Erabia and by the exposure of this part to the dominant swells and also the human activities like used the beach for amusement activities (Beach Ball competition and other). Beach profile observations results show accumulation in the subaerial beach and erosion in the lower part of the foreshore. The study on two different time scales adopted in this paper, allowed us to understand longshore and cross-shore sedimentary mobility.

**Keywords:** sandy beach, GIS tools, DSAS, DGPS, longshore drift, cross-shore.

### INTRODUCTION

Sandy beaches are dynamic systems in constant evolution due to their interaction with waves, tides, wind, and ocean currents, and react rapidly to natural forces either by accretion or retreat (Sherman & Bauer, 1993; Snoussi et al., 2018; Tao et al., 2022). In many areas of the world's oceans, it has been demonstrated that projections of wind-driven wave variations caused by climate change are significant (Hemer et al., 2013) The projected wind waves' potential coastal effects are anticipated to worsen as mean sea level rise accelerates, which will exacerbate the effects of extreme events and coastal flooding (Amores & Marcos, 2020).

El Jadida Beach is a sandy beach of low altitude that constitutes a kind of enclave located between the port of El Jadida and rocky outcrops. It is influenced by natural and anthropic factors that are reflected in the impact of marine forcing agents (wind, swells, tide, storms), geomorphological factors such as the rocky plain which breaks the swell force, installations like the harbor breakwater, which affects the sediments dynamic, as well as the impact of tourism, particularly during the summer, when sand is used for amusement activities (Beach Ball competition).

However, El Jadida beach is a destination that attracts thousands of visitors every year. It greatly impacts the city's economy, especially the

tourism industry, which brings in a lot of revenue to boost the economy. Over the last few years, we have observed the loss of sand from the beach, which continues to increase.

Sand is shifted along beaches by both marine (swell, tide and currents) and weather conditions, mainly wind. Such movement occurs along the beach (longshore) and in profile (cross-shore). To understand this sand movement at the El Jadida beach, we carried out a study on two different time scales: a fifty-five years (1963–2018) shoreline evolution study, using aerial photos and satellite images, (Wernette et al., 2017; El Khalidi, 2017; Minoubi et al., 2018; Hakkou et al., 2018; El Khalidi et al., 2021) and two-years (2017–2019) morphological beach study (Minoubi et al., 2013; El Khalidi, 2017; Ariffin et al., 2019).

### STUDY AREA

El Jadida beach (X: -8.5007116; Y: 33.2316326) is located on the Moroccan Atlantic coast at 15.5 km south of Oued Oum Erabia. It is a beach of 1.6 Km limited; on its northwest side by the harbor seawall and on the southeast side by the beginning of rocky outcrops. This beach consists of a subaerial beach, slightly wide (>20 m) to the east and northwest, narrow (<14 m) along the rest of its length, which makes up its middle, and finally bordered toward the south-west (land side) by several small cabins intended for the summers.

In front of the subaerial beach, the foreshore reaches 200 meters wide at low tide. The foreshore is characterized by rocky outcrops in its lower part, toward the port. The sands that make up this beach can be carried towards the city by strong winds and sometimes overflow the wall that runs along the beach during periods of severe swells.

According to Chaibi (2003), El Jadida Beach’s sands are fine, well-classified to very well-classified sands with a heterogeneous index of dissymmetry that displays values ranging between an almost symmetrical and a strongly asymmetrical trend towards the coarse.

The direction of the littoral drift oriented North-South is created by NNW swells, and due to north-west swells, a littoral drift that faces south to north is created (Chaibi, 2003). The winter season is marked by an increase in swell height and duration, which leads to a high frequency of storms; however, the summer season is less agitated (Chaibi, 2003). In contrast, spring is a time when agitation and calm are in transition.

In coastal dynamics, swells play a significant role in transport and erosion, primarily through their breaking. 90% of the time, NNW and WNW swells are the most frequent. The most effective swells are those with heights over 2 m, they have a frequency of over 40% of the time (Figure 1). El Jadida’s littoral is characterized by the predominance of moderate winds from the N, NE, NW and SW sectors, while the strong winds (11 to 16 m/s) always come from the W and SW sectors.

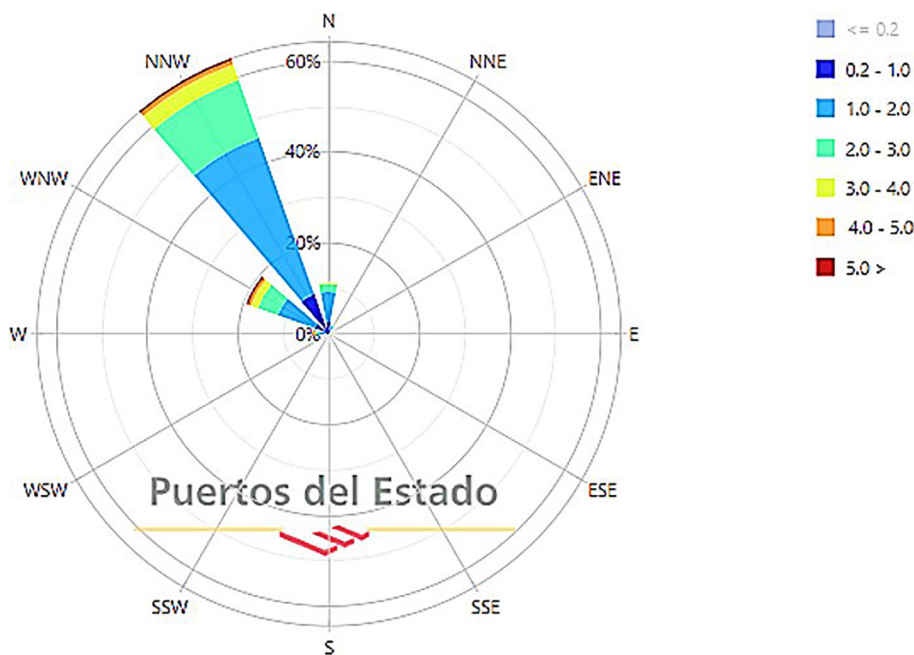


Figure 1. Rose of swells for the period between 1958 and 2023 (Puertos website)

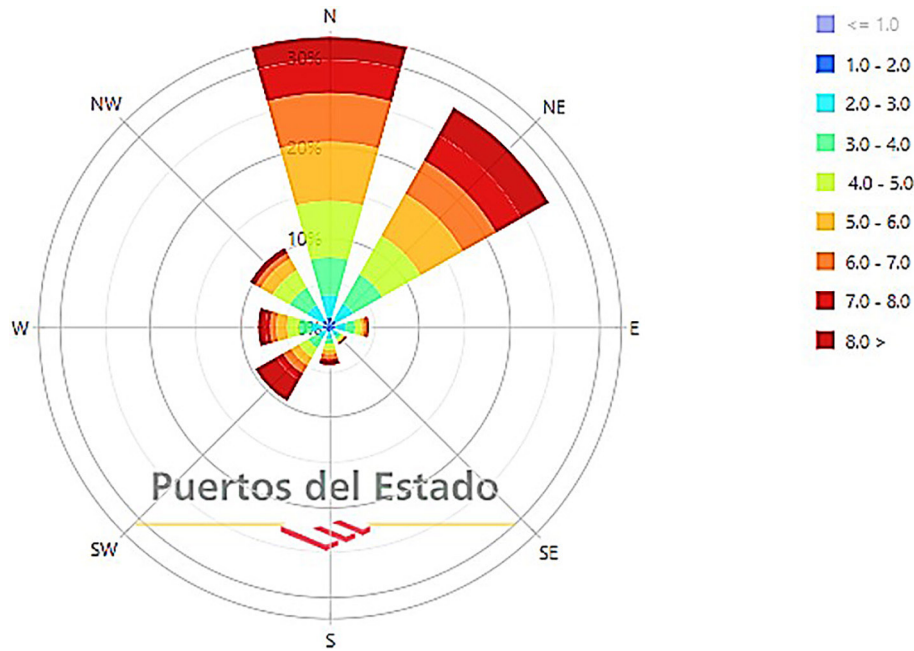
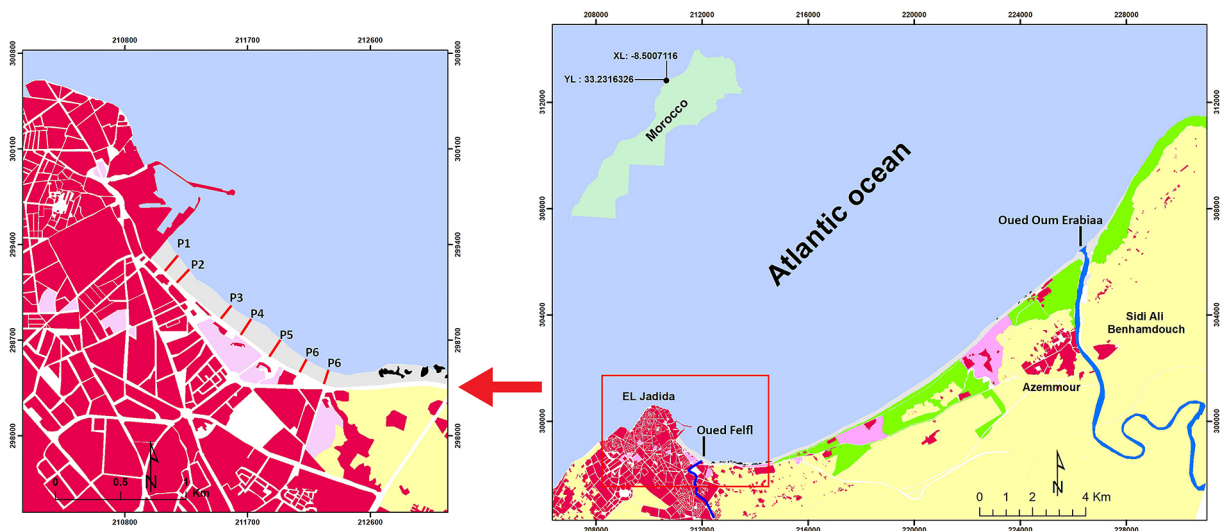


Figure 2. Wind roses for the period between 1958 and 2023 (Puertos website)



**Legend**  
Land use / Land Cover ( according to corine land cover classification)

Urbanized areas	Forest
Agricultural Areas	Coastal dunes / Beach
Green urban areas	Bare rock

Figure 3. Map of the study area location

## MATERIALS AND METHODS

### Fifty-five years (1963–2018) shoreline changes

The methodology adopted in this study aims to identify the Spatiotemporal evolution of a sandy beach; based on coastline dynamics and morphological variability. The fifty-five years (1963–2018) shoreline evolution was measured

using topographic maps (2010), aerial photos, and satellite images (1963, 1970, 1982, 2010, and 2018), covering a period of 55 years (Table 1).

### Shoreline analysis

The coastline dynamics were determined by computer-assisted photo interpretation; a method approved by several authors (Shoshany & Degani, 1992; Mapping & Moore, 2000; Salim et al.,

**Table 1.** Data used for monitoring a diachronic analysis of the shoreline along the El Jadida beach

Data type	Date	Scale	N° of Photos and maps used	Pixel size	Data sources
Aerial photos	04/10/1963	1/40000	1	1.1	ANCFCC*
	07/26/1970	1/50000	1	4.42	ANCFCC
	05/01/1982	1/30000	1	2.7	ANCFCC
	04/20/2010	1/25000	1	1.9	ANCFCC
Satellite images	05/15/2018	1/35000	2	1.24	Google Earth
Topographic map	04/12/2011	1/25000	3	1.09	ANCFCC

Note: \*National Agency for the Land Conservation of Cadastre and Cartography.

2021; Lollino et al., 2021). This process is based on the following steps: image georectification, reference line selection, coastline digitizing and error estimation, and calculation of the coastline change rate.

The photos were scanned in a resolution of 300 DPI in the TIFF format and then georeferenced using ArcGIS 10.2 software in the Lambert Conformal Conic reference system zone 1 datum Merchich spheroid Clarke 1880. The georeferencing was done from the topographic maps while matching the aerial photos to the topographic maps (Dolan et al., 1980; Anders and Byrnes, 1991; Crowell et al., 1991; Moore, 2000; Menie Ovono, 2010; Gaillot & Chaverot, 2001; Chaibi, 2003; Dehouck, 2006; Menie Ovono, 2010; Faye, 2010; El Khalidi, 2017, Minoubi et al., 2018). In the present work, between 20 and 50 ground-control were captured per image, which partly minimizes the margin of error (RMS) calculated by the software, where it is necessary to calibrate images from various missions to examine the degree of overlap between the contours and notable features (roads, developments, or other features). In the context of a diachronic study using photo interpretation, it is crucial to choose a common reference line across all of the images (Moussaid et al., 2015) In this paper, the reference line chosen was the high-water line (Minoubi et al., 2018; Hakkou et al., 2018; El Khalidi et al., 2021).

After digitizing the Shorelines, their change rate was calculated using the Digital Shoreline Analysis System (DSAS) developed by the United States Geological Survey (USGS); By generating transects from a baseline, intersecting

with the shorelines. On a distance of 1.6 Km, the DSAS generated 159 transects, with a spacing of 10 m and 170 m in length.

### Error estimation

Shoreline mapping is impacted by various sources of uncertainty, which in turn affects the shoreline change rate (Fletcher and al., 2003). In this regard, four distinct types of errors related to data quality and measurement accuracy have been identified. Namely the pixel error ( $Ep$ ), the error related to the georeferencing (Root Mean Square Error (RMSE)) ( $Er$ ), the reference line's digitization error ( $Ed$ ), and the high-water line oscillation error ( $Ev$ ). These different errors are considered in equation (1) ESP, which expresses the total error calculated for each period. This has been annualized to give equation (2)  $E\alpha$ , which is the error estimate over the whole study period.

$$ESP = \sqrt{Ed^2 + Er^2 + Ep^2 + Ev^2} \quad (1)$$

$$E\alpha = \sqrt{\frac{Esp1^2 + Esp2^2 + Esp3^2}{Time}} \quad (2)$$

The calculation's output indicates that the value of total shoreline position error is  $\pm 8$  m and the annualized transect error during a period of 55 years is  $\pm 0.3$  m/year.

### Rate of shoreline change

In this study, the shoreline change rate was calculated using the EPR (The end-point rate) and

**Table 2.** Estimated measurement errors for each shoreline data source

Measurement errors (m)	Different shoreline data sources				
	1963	1970	1982	2010	2018
Total shoreline position error (m) $Esp$	6.8	8.3	9.5	7.3	8
Annualized transect error (m/year) $E\alpha$	0.3				

LRR (linear regression rate) index. The end point rate (EPR) is calculated by dividing the distance of shoreline movement by the time elapsed between the oldest and the most recent shoreline. A linear regression rate-of-change statistic can be determined by fitting a least-squares regression line to all shoreline points for a transect. The positive and negative EPR, and LRR values indicated areas of accumulation and erosion respectively.

### Two-years profiles changes

To determine the morphological variability of the beach studied, seven beach profiles were monitored regularly to analyze its seasonal variability between November 2017 and January 2019 (Figure 1).

Before starting our regular follow-up missions, preparation in advance was made in order to facilitate the following missions. Specifically, the positioning of fixed markers on the cornice to serve as each profile's initial starting point, and the location of a reference point with known coordinates (X, Y, Z) to calibrate the (DGPS).

### Topographic surveys and data analysis

The DGPS station is positioned on the above-mentioned reference point, taking care of its configuration and the flatness of the measurement surface. The beach profiles were conducted during low tide, from the ledge's fixed markers to the low foreshore. Trough Excel, represented graphically as superimposed curves indicating the seasonal variability of El Jadida Beach.

## RESULTS AND DISCUSSION

Calculating the shoreline is one of the key elements to identify coastal accretion or/and erosion and to studying coastal morphodynamics (Armenio et al., 2019; Baig et al., 2020). Therefore, it is crucial to accurately characterize and monitor the coastline in order to comprehend coastal processes and the dynamic behavior of coastal features (El Khalidi et al., 2021). The outcome of the coastline's diachronic analysis using an automatic thresholding method is shown in Table 3 and Figure 4.

### Fifty-five years (1963–2018) shoreline changes

The DSAS results provided valuable information regarding the evolution of the coastline, by locating erosion and accretion zones over a 55-year (1963–2018). The El Jadida beach shows an accretion on its northern and southern parts with rates of 0.14 m/year and 0.07 m/year, respectively, and an erosion of the median part of -0.065 m/year. The site is shielded from wind erosion by a short wall (between 1 and 1.5 meters high) running the entire length of the beach (Chaibi, 2003). This wall disrupts and influences the aeolian sediment transfers that are from the sea to the land (Chaibi, 2003). In addition, this beach also benefits from natural protection thanks to the existence of some rocky outcrops in mid-tide that reduce the swell's effects (Chaibi, 2003).

The erosion in the middle of the beach can be explained by the fact that this part of the beach is

**Table 3.** Statistics of EPR and LRR with a confidence interval of 99.9%

Beach area		El Jadida Beach
Total number of transects		159
Coastline length (Km)		1.6
EPR	Mean mobility shoreline change (m/year)	0.03
	Maximum mobility shoreline change (m/year)	0.27
	Minimum mobility shoreline change (m/year)	-0.12
	Standard deviation of mobility (m/year)	0.07
	Total transect that records erosion	63
	Total transect that records accretion	96
LRR	Mean mobility shoreline change (m/year)	-0.1
	Maximum mobility shoreline change (m/year)	0.15
	Minimum mobility shoreline change (m/year)	-0.38
	Standard deviation of mobility (m/year)	0.13
	Total transect that record erosion	97
	Total transect that record accretion	62

less protected from swells, the aerial beach is narrowed and has a smooth slope, allowing the tide to wet 3 meters of the subaerial beach during a high tide, or even get to the cornice’s wall. The detour of oued Felfel, which pours before in the middle of the beach during floods. We can also point to the decrease in sediment transported by Oued Oum Erabia since the first dam was put into operation in the early thirties, as well as the recent narrowing of the Oued Oum Erabia mouth which further prevents sediments from reaching the ocean.

Beach erosion brought on by a decrease in sediment supply is a global phenomenon. For instance, the erosion of Calvi Bay in Corsica is

linked to the reduction of gravel and sand transported by the rivers of Figarella and Fiume Seccu (Gaillot & Piégay, 1999). Another study carried out on California beaches shows that the 500 dams built on the California coastal watershed, reduced 2.8 million m<sup>3</sup>/year equivalent to (25%) of the annual average sand and gravel flow, the factor that endangers the beaches, and long-term erosion is to be expected (Willis & Griggs, 2003).

**Two-years (2017–2019) profiles changes**

El Jadida beach is made up of a 190 m fore-shore and a 10 m to 30 m wide subaerial beach,

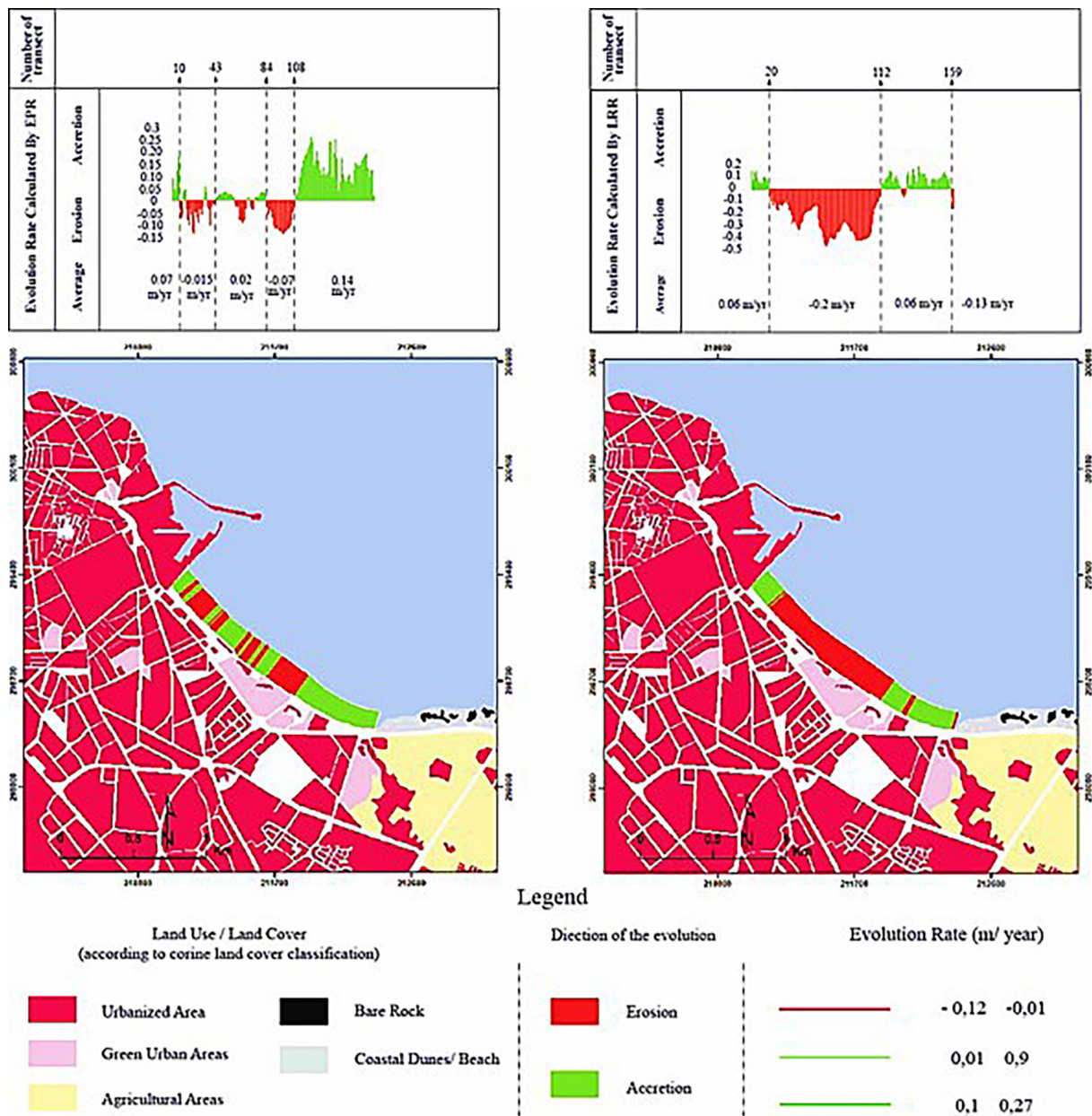


**Figure 4.** Shoreline evolution between 1963 and 2018 (erosion and accretion), calculated by the Linear Regression Rate (LRR) and End Point Rate (EPR) methods

which is characterized by the absence of a dune sedimentary stock, the only sedimentary sources come from the North East beaches (Chaibi, 2003). The morphology of the beach profiles is similar and, in some cases, identical, with a predominant concave shape.

The seasonal variability of the beach profiles revealed that the sand stock is very dynamic in this area (El Jadida beach), due to longitudinal and transversal transfers, caused by meteorological and marine actions (Chaibi, 2003). It also shows an accumulation characterizing the subaerial beach, the upper and middle foreshore, whilst erosion characterizes the lower foreshore.

*Profile 1*

The profile 1 shows a decreasing trend (Figure 5); morphological variations during the first three missions (November 2017, April 2018, and June 2018) show an erosion at the subaerial beach, high and mid foreshore with an accumulation at the low foreshore. Only the January 2019 mission shows the opposite of the previous missions. The volumetric balance shows a loss of -25,65 m<sup>3</sup>.

*Profile 2*

According to the numerous topographic surveys conducted at this station, this profile (Figure 5) has alternated between erosive and accumulative phases. The period between (November 2017 and April 2018) and the period between (June 2018 and January 2019) is marked by a fattening of the subaerial beach, the upper and mid foreshore with erosion at the lower foreshore, On the other hand, during the period between April 2018 and June 2018, this profile shows a fattening in the low foreshore, an erosion of the aerial beach, the high foreshore, and the mid foreshore. The sediment balance of these profiles is positive with an estimated gain of 115.047 m<sup>3</sup> (Figure 5).

*Profile 3*

This profile (Figure 6) shows a positive sediment budget of 36.40 m<sup>3</sup> (Figure 6). The superposition of the profiles of the first two missions (November 2017 and April 2018) shows an erosion that affects all its morphological units, followed by a fattening marking the 3rd and 4th missions with a slight erosion on the low foreshore and the subaerial beach.

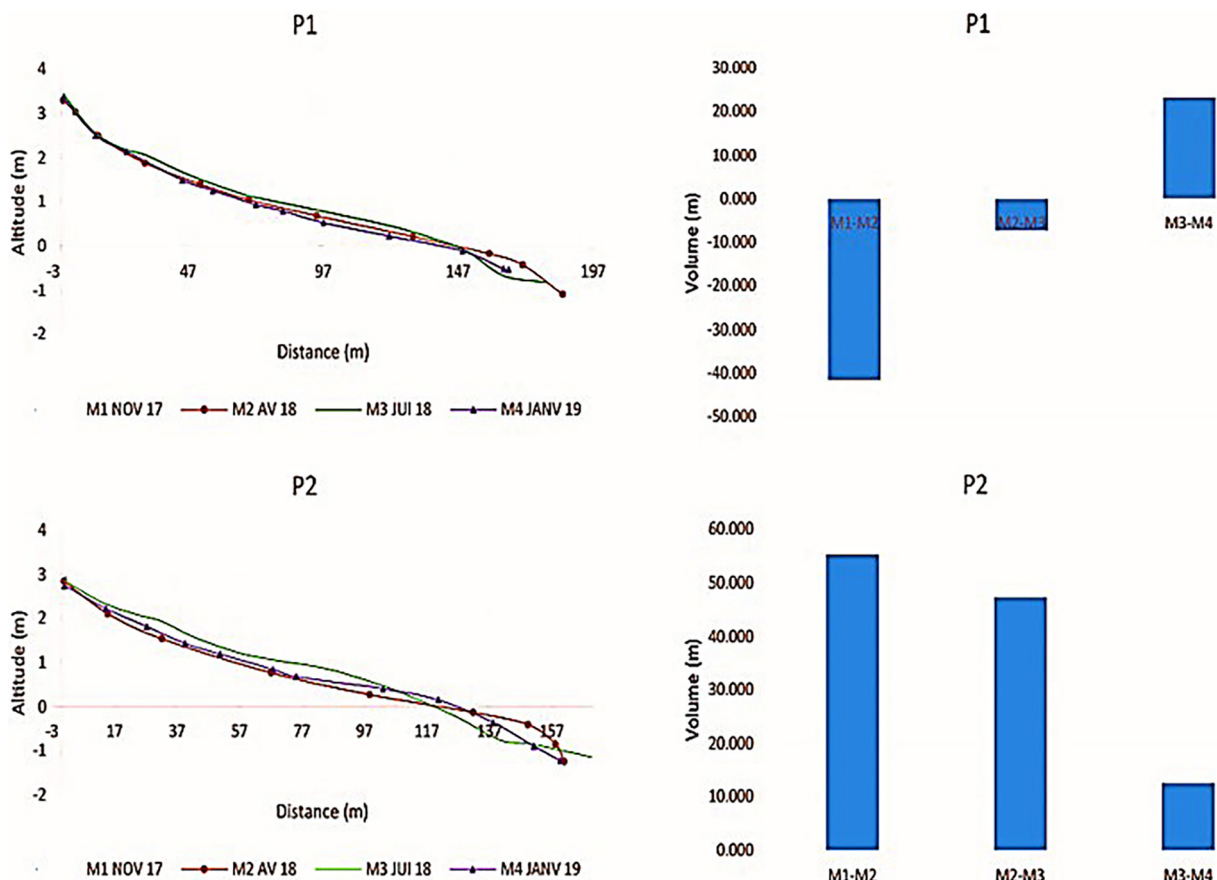


**Figure 5.** Morphological and volumetric variation of profiles 1 and 2 during the period between November 2017 and January 2019

Profile 4

The morphological evolution of this profile (Figure 6) shows an erosion that marks the period between (November 2017 and April 2018); a fattening at the low foreshore and erosion that affects the area between the subaerial beach and the mid-foreshore, followed by two episodes of fattening between (April 2018 and January 2019), the first of which features an erosion at the low foreshore and an accumulation covering the area between the subaerial beach and mid-tide. The same thing happened in the second episode, with a slight erosion at the low foreshore and subaerial beach. The volumetric balance indicates an increase of 8,68 m<sup>3</sup>.

Profile 5

Profile P5 (Figure 7) is characterized by a generalized erosion from November 2017 to April 2018, followed by a generalized fattening from April 2018 to January 2019. The sediment balance is 7.62 m<sup>3</sup>.

Profile 6

Profile P6 (Figure 7) is characterized by a developed aerial beach and a gently sloping

foreshore. The morphological variation between November 2017 and April 2018 reveals a negative sediment balance of -49.11 m<sup>3</sup> and a completely eroded foreshore, and a subaerial beach eroded on its high part and engraved on its low part. For the period between April 2018 and June 2018, we noticed a fattening on the whole foreshore, erosion on the low part of the subaerial beach, and a certain stability on its high part, with a 14.24 m<sup>3</sup> sediment balance. We observed an undulation of the two beach profiles between June 2018 and January 2019, with a series of fattening and erosion zones defining the entire profile with a sediment balance of 0.06 m<sup>3</sup>.

Profile 7

Profile P7 (Figure 7) is characterized by a developed subaerial beach, a straight foreshore with a break in the slope separating it from the aerial beach. The morphological variation during the four field missions shows an erosion episode followed by two fattening episodes. During the period between November 2017 and April 2018, erosion marked the entire profile except for a slight accumulation at the subaerial beach. All of

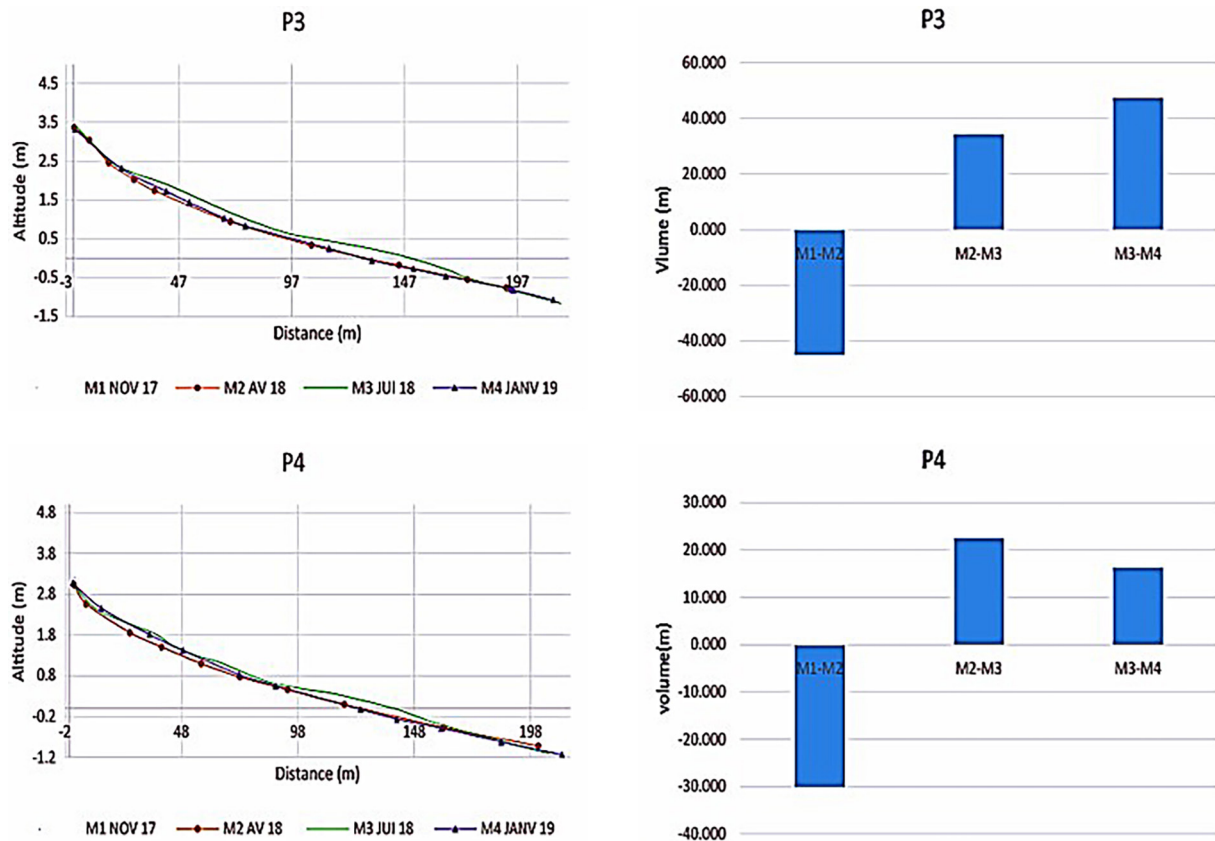


Figure 6. Morphological and volumetric variation of profiles 3 and 4 during the period between November 2017 and January 2019

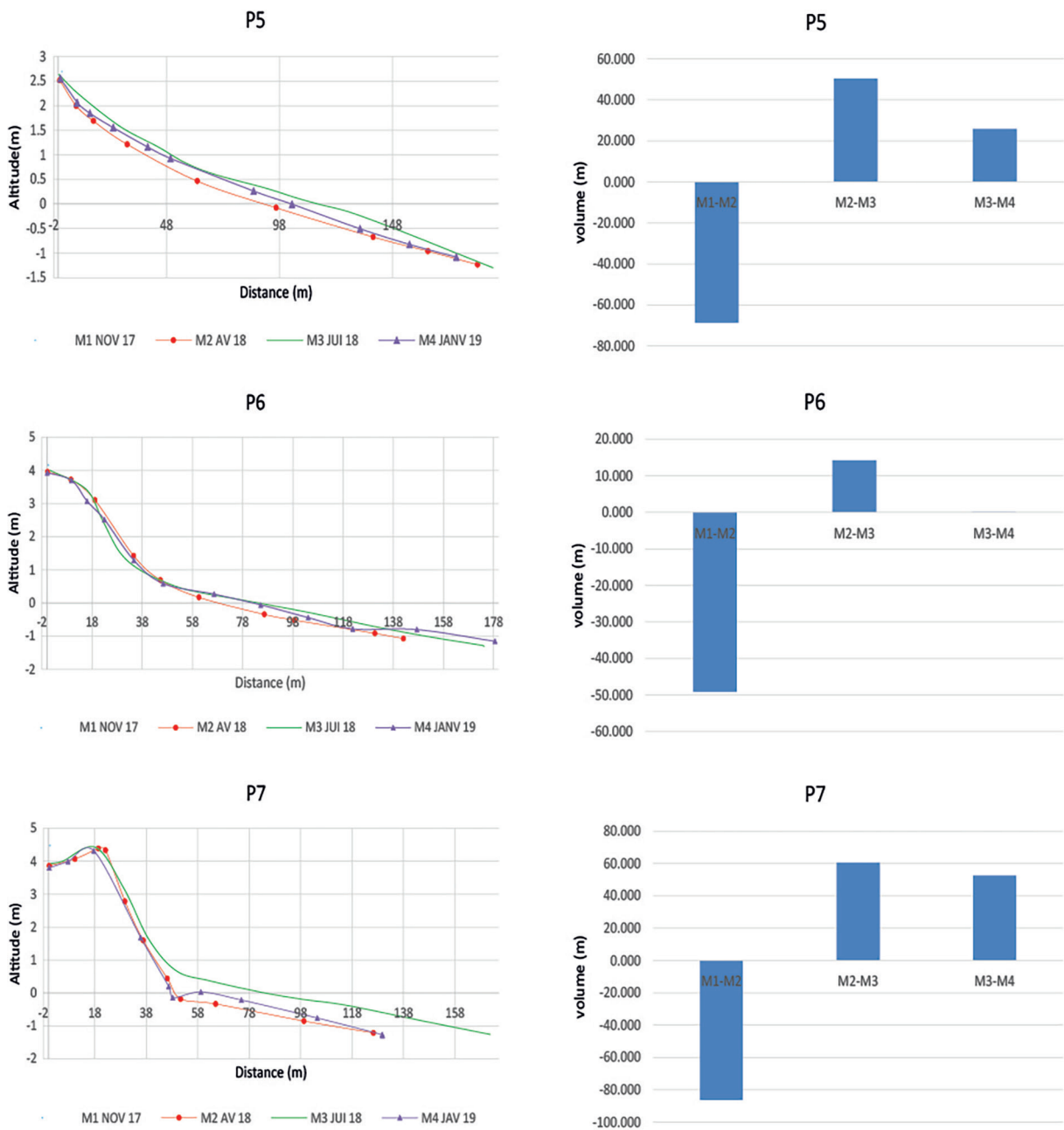


the morphological units of the profile show a fattening between April 2018 and June 2018, with the exception of a slight erosion of a small portion of the aerial beach. For the period between June 2018 and January 2019, it is the fattening that dominates the profile except for a small part of the subaerial beach. The current profile's volumetric balance is 26.81 m<sup>3</sup>.

The beach profiles of El-Jadida show a fattening characterizing the autumn and summer period (November 2017, July 2018). While, and erosion marks the winter and spring profiles (April 2018, January 2019). The total sediment budget shows

accumulation marking the subaerial beach, the upper and middle foreshore with an accretion rate varying between 0.13 m/yr and 0.21 m/yr, and a recession rate between -0.02 m/yr and -0.05 m/yr marking the lower foreshore.

Between November 2017 and January 2019, the morphological variation of the beach of El Jadida revealed a general tendency to accumulation, which can be explained by a number of combined factors, namely the direction of the swell, the configuration of the beach and geomorphological factors (rocky outcrops). The dominant swells are NNW, and the harbor breakwater is a



Figures 7. Morphological and volumetric variation of profiles 5, 6, and 7 during the period between November 2017 and January 2019

barrier that attenuates the intensity of the swell, the harbor breakwater also acts as a blocking device for longitudinal movements, and also the configuration of the beach, which is concave, allowing the dissipation of the energy of the swell, while the rocky outcrops to the south protect the beach by preventing the departure of sediments and favoring their accumulation at the subaerial beach.

## CONCLUSION

The aim of this study was to examine the morphodynamics of El Jadida beach and to understand the processes of its morphogenesis. In the case of El Jadida beach, it is a sandy mesotidal beach at a low altitude. Its dynamics are governed by marine and meteorological agents, in particular swell and wind. The most dominant swells are from NNW and WNW, while the dominant winds are from N, NE, NW, and SW. These variables and sometimes contradictory directions contribute to the attenuation of the impact of these factors.

The output of the fifty-five years (1963–2018) diachronic analysis reveals a beach with erosion in the middle and accretion at the edges. This is mainly due to the presence of the harbor breakwater to the NW and the rocky outcrops to the SE; acting as a barrier preventing the movement of sediments in both directions of the longshore drift. However, the erosion in the middle can be explained by the reduction of the sediment supply from the Oued Oum Erabia due to the construction of dams and by the exposure of this part to the dominant swells and also human activities like using the beach for amusement activities (Beach Ball competition and other).

Tow year observation missions of the morphological changes at El Jadida beach during the period from November 2017 to January 2019, reveals an accretion of subaerial beach, but an erosion of low foreshore. The beach profiles at the extremity of El Jadida beach show accretion due to the role played by the harbor wall (NW) and the rocky outcrops (SE) which block the sediments. However, the profiles have shown significant erosion at the low foreshore, but on the other hand an accumulation at the subaerial beach, this can be explained by the configuration of the beach which has a concave shape; its middle is exposed to swells.

The seasonal volumetric variation of beach profiles shows the alternation of periods of erosion and accretion. In the same profile, we have

two morphological units with opposite trends, which reverse in the next episode indicating a cross-shore drift.

The sediment balance of the beach profiles does not make it possible to determine the direction of a coastal transit, on the other hand, the combination of all the elements mentioned above makes it possible to deduce that the beach of El Jadida is a relatively closed sedimentary cell, marked by a littoral drift tending NW and NE which leads to an erosion of the environment and an accumulation at the edges of the beach.

The methods used in the present work, i.e. diachronic and morphological observations of El Jadida beach, give complementary results. However, in order to better understand the morphodynamics of this beach, we suggest a monitoring using DGPS, with regular time intervals between missions, combined with the collection of sand samples for granulometric analysis, which will allow us to know the origin of the sands and to determine the direction of the littoral transit.

## REFERENCES

1. Amores, A., Marcos, M. 2020. Ocean swells along the global coastlines and their climate projections for the twenty-first century. *Journal of Climate*, 33(1), 185–199. <https://doi.org/10.1175/JCLI-D-19-0216.1>
2. Anders, F.J., Byrnes, M.R. 1991. Accuracy of Shoreline Change Rates as Determined from Maps and Aerial Photographs. *Shore and Beach*, 59, 17–26.
3. Ariffin, E.H., Sedrati, M., Akhir, M.F., Norzilah, M.N.M., Yaacob, R., Husain, M.L. 2019. Short-term observations of beach Morphodynamics during seasonal monsoons: two examples from Kuala Terengganu coast (Malaysia). *Journal of Coastal Conservation*, 23(6), 985–994. <https://doi.org/10.1007/s11852-019-00703-0>
4. Armenio, E., De Serio, F., Mossa, M., Petrillo, A.F. 2019. Coastline evolution based on statistical analysis and modeling. *Natural Hazards and Earth System Sciences*, 19(9), 1937–1953. <https://doi.org/10.5194/nhess-19-1937-2019>
5. Fletcher, C., Rooney, J., Barbee, M., Lim, S.C., Richmond, B. 2003. Mapping shoreline change using digital orthophotogrammetry on Maui, Hawaii. *Journal of Coastal Research*, 106–124.
6. Baig, M.R.I., Ahmad, I.A., Shahfahad, T.M., Rahman, A. 2020. Analysis of shoreline changes in Vishakhapatnam coastal tract of Andhra Pradesh,

- India: an application of digital shoreline analysis system (DSAS). *Annals of GIS*, 26(4), 361–376. <https://doi.org/10.1080/19475683.2020.1815839>
7. Chaibi, M. 2003. Dynamique sédimentaire et morphogénèse actuelle du littoral d'El Jadida (Maroc).
  8. Crowell, M., Leatherman, S.P., Buckley, M.K. 1991. Historical shoreline change: Error Analysis and Mapping Accuracy. *Journal of Coastal Research*, 7(3), 839–852.
  9. Dolan, R., Hayden, B.P., May, P., May, S. 1980. The reliability of shoreline change measurements from aerial photographs. *Shore and Beach*, 48, 22–29.
  10. El Khalidi, K., Bourhili, A., Bagdanavičiūtė, I., Minoubi, A., Hakkou, M., Zourarah, B., Maanan, M. 2022. Coastal land use and shoreline evolution along the Nador lagoon Coast in Morocco. *Geocarto International*, 37(25), 7445–7461. <https://doi.org/10.1080/10106049.2021.1974958>
  11. El Khalidi, K., Maanan, M., Hakkou, M., Nafouri, I., Zourarah, B. 2020. Influence of the margin of error related to the use of aerial photographs on the interpretation of the shoreline changes: evidence from three case studies from the Atlantic coast of Morocco. *International Journal of Advanced Research in Engineering and Technology (IJARET)*, 11(12), 457–467. <https://doi.org/10.34218/IJARET.11.12.2020>
  12. Faye, I.B.N. 2010. Dynamique du trait de côte sur les littoraux sableux de la Mauritanie à la Guinée-Bissau (Afrique de l'Ouest): Approches régionale et locale par photo-interprétation, traitement d'images et analyse de cartes anciennes, 1, 321.
  13. Gaillot, S., Chaverot, S. 2001. Méthode d'étude des littoraux à faible évolution. Cas du delta du Golo (Corse) et du littoral du Touquet (Pas de Calais) en France, *Géomorphologie: Relief, Processus, Environnement*, 7(1), 47–54. <https://doi.org/10.3406/morfo.2001.1086>
  14. Gaillot S., Piégay H. 1999. Impact of Gravel-Mining on Stream Channel and Coastal Sediment Supply: Example of the Calvi Bay in Corsica (France). *Journal of Coastal Research*, 15(3), 774–788.
  15. Hakkou, M., Maanan, M., Belrhaba, T., El Khalidi, K., El Ouai, D., Benmohammadi, A. 2018. Multi-decadal assessment of shoreline changes using geospatial tools and automatic computation in Kenitra coast, Morocco. *Ocean and Coastal Management*, 163, 232–239. <https://doi.org/10.1016/j.ocecoaman.2018.07.003>
  16. Hemer, M.A., Katzfey, J., Trenham, C.E. 2013. Global dynamical projections of surface ocean wave climate for a future high greenhouse gas emission scenario. *Ocean Modelling*, 70, 221–245. <https://doi.org/10.1016/j.ocemod.2012.09.008>
  17. El Khalidi, K. 2007. Morphological and diachronic study of the lagoon of Sidi Moussa, Morocco. *Terra et aqua*, 106, 3.
  18. Lollino, P., Pagliarulo, R., Trizzino, R., Santaloia, F., Pisano, L., Zumpano, V., Perrotti, M., Fazio, N.L. 2021. Multi-scale approach to analyse the evolution of soft rock coastal cliffs and role of controlling factors: A case study in South-Eastern Italy. *Geomatics, Natural Hazards and Risk*, 12(1), 1058–1081. <https://doi.org/10.1080/19475705.2021.1910351>
  19. Moore, L.J. 2000. Shoreline mapping techniques. *Journal of coastal research*, 111–124.
  20. Menie Ovono, Z. 2010. Evolution de la flèche mandji de l'holocène à l'actuel. Analyse et cartographie du risque côtier. these de doctorat, Université de Nantes France, 298.
  21. Minoubi, A., El Khalidi, K., Chaibi, M.M., Zourarah, B., Poizot, E., Amrouni, O. 2013. Variation Morphosedimentary seasonal variation and the impact of the January 2009 storm on the coast of Safi, Morocco. *Science Lib Editions Mersenne*, 5(130202), 1–23.
  22. Minoubi, A., El Khalidi, K., Chaibi M., Zourarah, B., Ayt Ougougdal, M., Poizot, E., Mear, Y. (2018). Impact des ouvrages portuaires sur l'évolution du trait de côte de la baie de Safi (littoral atlantique-Maroc). *Revue Marocaine de Géomorphologie*, 2, 18–35.
  23. Moore, L.J. 2000. Shoreline mapping techniques. *Journal of Coastal Research*, 111–124.
  24. Moussaid, J., Fora, A.A., Zourarah, B., Maanan, M., Maanan, M. 2015. Using automatic computation to analyze the rate of shoreline change on the Kenitra coast, Morocco. In *Ocean Engineering*, 102, 71–77. Elsevier Ltd. <https://doi.org/10.1016/j.oceaneng.2015.04.044>
  25. Salim, F.Z., El Habti, M.Y., Lech-Hab, K.B.H., El Arrim, A. 2021. A diachronic study of the Mediterranean coastline: A geometric approach. *E3S Web of Conferences*, 234. <https://doi.org/10.1051/e3sconf/202123400039>
  26. Sherman, D.J., Bauer, B.O. 1993. Dynamics of beach-dune systems. *Progress in Physical Geography*, 17(4), 413–447. <https://doi.org/10.1177/030913339301700402>
  27. Shoshany, M., Degani, A. 1992. Shoreline detection by digital image processing of aerial photography. *Journal of Coastal Research*, 29–34.
  28. Snoussi, M., Khalfaoui, O., Flayou, L., Kasmi, S., Raji, O. 2018. Can ICZM help the resilience of disappearing beaches in the face of climate change? In *Advances in Science, Technology and Innovation*. Springer Nature, 29–30. [https://doi.org/10.1007/978-3-319-70548-4\\_11](https://doi.org/10.1007/978-3-319-70548-4_11)
  29. Tao, H.C., Hsu, T.W., Fan, C.M. 2022. Developments of Dynamic Shoreline Planform of

- Crenulate-Shaped Bay by a Novel Evolution Formulation. *Water*, 14(21), 3504. <https://doi.org/10.3390/w14213504>
30. Wernette, P., Shortridge, A., Lusch, D.P., Arbogast, A.F. 2017. Accounting for positional uncertainty in historical shoreline change analysis without ground reference information. *International Journal of Remote Sensing*, 38(13), 3906–3922. <https://doi.org/10.1080/01431161.2017.1303218>
31. Willis, C.M., Griggs, G.B. 2003. Reductions in fluvial sediment discharge by coastal dams in California and implications for beach sustainability. *Journal of Geology*, 111(2), 167–182. <https://doi.org/10.1086/345922>